

A dynamical theory for one-dimensional fermions with strong two-body losses: universal non-Hermitian Zeno physics and spin-charge separation

Lorenzo Rosso,¹ Alberto Biella,^{2,1} Jacopo De Nardis,³ and Leonardo Mazza^{1,*}

¹*Université Paris-Saclay, CNRS, LPTMS, 91405 Orsay, France*

²*INO-CNR BEC Center and Dipartimento di Fisica, Università di Trento, 38123 Povo, Italy.*

³*Laboratoire de Physique Théorique et Modélisation, CNRS UMR 8089, CY Cergy Paris Université, 95302 Cergy-Pontoise Cedex, France*

We study an interacting one-dimensional gas of spin-1/2 fermions with two-body losses. The dynamical phase diagram that characterises the approach to the stationary state displays a wide quantum-Zeno region, identified by a peculiar behaviour of the lowest eigenvalues of the associated non-Hermitian Hamiltonian. We characterise the universal dynamics of this Zeno regime using an approximation scheme based on an effective decoupling of charge and spin degrees of freedom, where the latter effectively evolve in a non-Markovian way according to a non-Hermitian Heisenberg Hamiltonian. We present detailed results for the time evolution from initial states with one particle per site with either incoherent and antiferromagnetic spin order, showing how the two non-equilibrium evolutions build up drastically different charge correlations.

Introduction — Losses are ubiquitous in ultra-cold gases and in several situations their interplay with quantum physics is at the basis of a remarkable phenomenology. They can be used to detect quantum coherence and the onset of Bose-Einstein condensation [1–3], to stabilize quantum Hall states [4], to cool the gas [5–7], or even to drive it through phases which violate the equilibrium thermodynamic Tan’s relation [8].

Several experiments have addressed the general problem of the dynamics of correlated one-dimensional quantum gases in the presence of two-body losses, both for bosons [9–15] and for fermions [16–18]; theory works have further inspected these setups [19–26]. In the presence of spinful gases, the stationary states can be highly non-trivial, and an incoherent mixture of entangled Dicke states is stabilised by losses, possibly useful for metrological purposes [27–30]. Moreover, when losses are strong, the quantum Zeno (QZ) regime sets in, and a counter-intuitive increase of the gas lifetime takes place as the loss rate is augmented [31–43]. Whereas a theory of the dynamics of spinless bosonic gases in this regime has been developed [22, 24], the same is not true for spinful fermionic gases: this constitutes a fundamental hurdle both for the exploitation of the entangled stationary states and for the interpretation of existing experiments.

In this letter we present a dynamical theory for a spin-1/2 fermionic gas in the presence of strong elastic or inelastic interactions (losses). The study of how stationarity is approached allows us to identify a QZ regime emerging when the system is strongly-dissipative or strongly-interacting. For a given initial state, a rescaling of times shows that the QZ dynamics is universal; this property is at the heart of a simple theory that we develop to characterise the time-evolution of local observables. Spin-charge separation takes place and spin degrees of freedom are dissipatively cooled according to a slow non-Hermitian Heisenberg Hamiltonian, and we show that the cooling rate is set by the charge properties of the

gas. Different approximation schemes are discussed for the charge of the gas, and we propose a simple method to account for quantum correlations. By considering two experimentally-relevant initial states, and by predicting the dynamics of several experimental signatures, among which the density of the gas, its magnetic correlations, and its momentum distribution function, we expect to trigger a novel generation of quantitative experimental studies.

The model — We consider a gas of spin-1/2 fermions trapped in a one-dimensional (1D) optical lattice and prepared with one particle per site; several spin configurations will be considered. At time $\tau = 0$ the optical lattice is lowered so that particles can tunnel to neighbouring minima; two-body losses can take place when two particles occupy the same site.

Our goal is to characterise the dynamics of the gas, which is described by a Lindblad master equation for ρ , the density matrix of the system:

$$\dot{\rho} = \mathcal{L}[\rho] = -\frac{i}{\hbar}[H, \rho] + \sum_j L_j \rho L_j^\dagger - \frac{1}{2}\{L_j^\dagger L_j, \rho\}. \quad (1)$$

The 1D Hubbard Hamiltonian models the optical lattice in the single-band approximation:

$$H = -t \sum_{j,\sigma} (c_{j,\sigma}^\dagger c_{j+1,\sigma} + H.c.) + U \sum_j n_{j,\uparrow} n_{j,\downarrow}; \quad (2)$$

two-body losses are described by the jump operators $L_j = \sqrt{\gamma} c_{j,\uparrow} c_{j,\downarrow}$. The $c_{j,\sigma}$ operators satisfy canonical anticommutation relations (j labels the site and σ the spin) and the density operator is $n_{j,\sigma} = c_{j,\sigma}^\dagger c_{j,\sigma}$; the hopping amplitude is t and U is the interaction parameter, γ is the loss rate. The problem depends on two effective parameters: $\hbar\gamma/(2t)$ and U/t . The spin of the gas is described by

$$\vec{S} = \sum_j \vec{S}_j = \frac{\hbar}{2} \sum_j \sum_{\tau,\tau'} c_{j,\tau}^\dagger \vec{\sigma}_{\tau\tau'} c_{j,\tau'}, \quad (3)$$

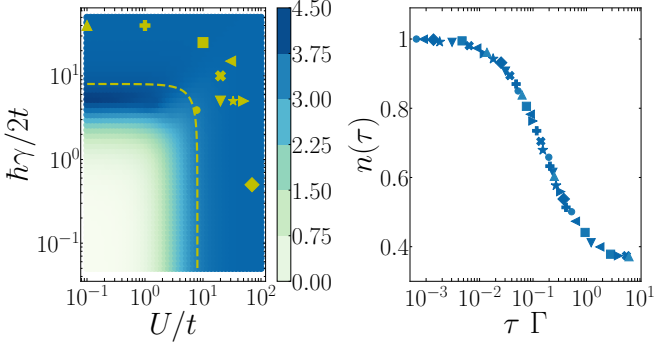


FIG. 1. (Left) Color plot of ζ defined in Eq. (4) in the parameter space. The green dashed line is the circumference with radius $|\xi| = 8.0$ and is proposed as an approximate bound for the QZ regime. The exact diagonalisation is performed for $N = L = 8$ in the sector with $S_z = 0$; the sum is arbitrarily restricted to 50 eigenvalues. (Right) Universal QZ dynamics for the density of the gas: different curves correspond to different points in the QZ region of the parameter space. The collapse is obtained by rescaling time with Γ . Simulations are performed for $L = 6$.

where $\vec{\sigma}$ are the three Pauli matrices. The dynamics conserves the spin, as it can be deduced from the jump operators, that annihilate a spin singlet [27].

Non-Hermitian Hamiltonian — In order to characterise the long-time dynamics and the approach to stationarity in the whole parameter space, we consider the non-Hermitian Hamiltonian associated to the problem [44], $\tilde{H} = H - (i\hbar/2) \sum_j L_j^\dagger L_j$, which in our case is just the Hubbard model with adimensional complex interaction $\xi = U/t - i\hbar\gamma/(2t)$. We diagonalise \tilde{H} using the package QuSpin [45, 46]; the analysis of the complex eigenvalues shows the existence of two well-defined regions. In the weakly-dissipative and weakly-interacting regime appearing approximately for $|\xi| \lesssim 1.7$, the imaginary part of the eigenvalues increases linearly with γ , so that the lifetime of the gas decreases by increasing the loss rate (see supplementary material (SM) [47] and [30] for a study of the dynamics).

In the QZ regime, appearing approximately for $|\xi| \gtrsim 8.0$, there is a group of eigenvalues whose imaginary part decreases as $\hbar\gamma/|\xi|^2$, so that the lifetime of the gas increases with γ or with U . To quantify this behaviour, we define the ratio

$$\zeta = \frac{\sum_i \Im[\lambda_i]}{\hbar\gamma/|\xi|^2}, \quad (4)$$

where λ_i are the eigenvalues of \tilde{H} and the sum is restricted to a set of eigenvalues with smallest imaginary part (in absolute value), which are those that determine the long-time dynamics. The plot in Fig. 1(left) shows that ζ has a clear finite value in a wide parameter region, a result that is more general than the standard quantum Zeno effect, because it takes place also for small γ .

In general, this increased lifetime follows from the absence of doubly-occupied lattice sites, which can be the consequence of strong elastic or inelastic interactions; at long times, the gas is composed of long-lived *hard-core* fermionic particles which never occupy the same site in pairs.

We verify the existence of the QZ regime also in the quantum dynamics by performing a simulation of the master equation (1) with the package QuTiP [48, 49]. As a simple example, we initialize a Néel state with one particle per site and staggered spin structure, $|\Psi_N\rangle = |\dots \uparrow\downarrow\uparrow\downarrow\dots\rangle$, and evolve it with parameters such that $|\xi| > 8.0$: the results are shown in Fig. 1(right) and the densities $n(\tau)$ collapse by rescaling the time with the typical Zeno rate $\Gamma = \gamma/|\xi|^2$.

Infinite spin temperature — We begin by developing our theory considering the initial state that has exactly one particle per site and infinite spin temperature, that is, a fully-incoherent spin state. Given its high mixedness, we adopt this simple mean-field (MF) equation, first proposed in Refs. [18, 19]:

$$\frac{d}{d\tau} n(\tau) = -\Gamma g^{(2)}(\tau) n(\tau)^2, \quad (5)$$

where $g^{(2)}(\tau)$ is the nearest-neighbour spin correlation function:

$$g^{(2)}(\tau) = \frac{1}{L} \sum_i \left(\frac{\langle n_i n_{i+1} \rangle_\tau}{\langle n_i \rangle_\tau \langle n_{i+1} \rangle_\tau} - \frac{4}{\hbar^2} \frac{\langle \vec{S}_i \cdot \vec{S}_{i+1} \rangle_\tau}{\langle n_i \rangle_\tau \langle n_{i+1} \rangle_\tau} \right). \quad (6)$$

The problem posed by Eq. (5) is to understand the dynamics of $g^{(2)}(\tau)$; in Ref. [18] an approximate functional formula has been proposed to fit the dynamics; here, we rather present a microscopic dynamical theory without fit parameters based on the notion of many-body dissipative spin cooling (DSC).

In order to proceed with the DSC theory, we decouple the spin and charge sectors, and propose an ansatz for the density matrix that is a product of the two: $\rho(\tau) = \rho_c(\tau) \otimes \rho_s(\tau)$. This spin-charge separation is motivated by the well-known results for the hardcore-fermion (HCF) Hamiltonian (corresponding to the $U \rightarrow \infty$ Hubbard regime [50]), recently extended in Ref. [28] to the non-Hermitian case.

Several methods have been proposed to deal with the spin-charge separation of HCFs [51–57]; we use here one that is due to Zvonarev et al. [58]. The Hilbert space of N HCFs on a lattice of length L is mapped to a one-dimensional model of N spinless fermions on a lattice of length L tensored with a spin-1/2 chain of length N . For instance, the state with $L = 4$ sites and $N = 2$ particles $|\uparrow\circ\circ\downarrow\rangle$ is mapped onto the state $|\bullet\circ\circ\bullet\rangle \otimes |\uparrow\downarrow\rangle$. The spin chain carries information about the spin of each particle in an ordered way, from left to right. We introduce the canonical fermionic operators a_j and the spin operators $\vec{\Sigma}_\ell$ in order to describe the charge and spin

degrees of freedom that we just introduced. Whenever dealing only with charge properties, relations between the two languages are simple: $a_j^\dagger a_j$ corresponds to $n_j = n_{j,\uparrow} + n_{j,\downarrow}$; for this reason, we will use the notation n_j both in the original fermionic language and in the novel HCF one. Exact mappings for spin properties instead are analytically intractable and thus we will make use of simpler approximated relations as discussed below.

Coherently with the mean-field spirit of Eq. (5), we propose that density-density correlations can be approximated as $\langle n_j n_{j+1} \rangle_\tau = \langle n_j \rangle_\tau \langle n_{j+1} \rangle_\tau = n^2(\tau)$. Obviously, this simplifies the expression for the $g^{(2)}(\tau)$: for instance, the first term appearing in Eq. (6) becomes exactly 1. A simplification of the second term is also possible if we assume translational invariance and that:

$$\vec{S}_i \cdot \vec{S}_{i+1} \approx n_i n_{i+1} \times \frac{1}{N} \sum_{\ell} \vec{\Sigma}_{\ell} \cdot \vec{\Sigma}_{\ell+1}. \quad (7)$$

The writing decouples exactly spin and charge operators so that its expectation value over the ansatz density matrix is easily taken; after some algebraic manipulation we obtain:

$$g^{(2)}(\tau) = 4\Pi(\tau), \quad \text{with} \quad \Pi(\tau) = \frac{1}{N} \sum_{\ell} \langle \Pi_{\ell,\ell+1} \rangle. \quad (8)$$

Here $\Pi_{\ell,\ell+1} = 1/4 - \vec{\Sigma}_{\ell} \cdot \vec{\Sigma}_{\ell+1}/\hbar^2$ is the spin-singlet projection operator on two neighbouring sites of the spin chain, that represent the spins of the ℓ -th and $\ell+1$ -th particle; this expresses in a remarkably clear way the fact that only spin singlets are lost during the dynamics.

We propose an equation for $g^{(2)}(\tau)$ that is based on the non-Hermitian Heisenberg spin dynamics [28, 29]. We neglect the fact that losses change the number of particles and focus on the no-click dynamics of the model, that notoriously is that of a non-Hermitian Hamiltonian:

$$\dot{\rho}_s(\tau) \simeq -n(\tau)^2 \{ H_s, \rho_s(\tau) \}, \quad (9)$$

with H_s a simple ferromagnetic Heisenberg Hamiltonian, $H_s = -(\Gamma/2) \sum_j \vec{\Sigma}_j \cdot \vec{\Sigma}_{j+1}$. Note that it depends on charge properties via the prefactor describing the probability that two particles are sitting nearby.

The solution of this problem is simple: given the density matrix $\rho_s(0)$ describing the initial spin state, the normalised spin matrix must be of the form [59]:

$$\rho_s(\tau) = \frac{e^{-\beta_s(\tau)H_s} \rho_s(0) e^{-\beta_s(\tau)H_s}}{\text{Tr} [e^{-2\beta_s(\tau)H_s} \rho_s(0)]}. \quad (10)$$

The time-evolution of $\beta_s(\tau)$ incorporates the charge effects: $\beta_s(\tau) = \int_0^\tau n(\tau')^2 d\tau'$. The importance of non-Hermitian Heisenberg spin physics in lossy systems has already been suggested in Refs. [28, 29]; here we add that during this dissipative spin cooling the temperature flows at a rate that depends on the charge properties of the gas,

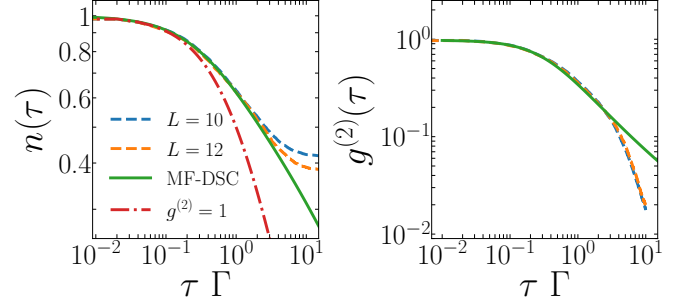


FIG. 2. Dynamics of the number of particles $n(\tau)$ (left) and of the spin correlation function $g^{(2)}(\tau)$ (right) for an initial maximally-mixed spin state. Dashed lines are obtained with numerical simulations of the master equation for $L = 10$ and $L = 12$. Solid green lines indicate the theoretical predictions obtained with our MF-DSC theory. Dashed-dotted lines indicate the naïve MF prediction of Eq. (5) with $g^{(2)} = 1$ kept constant during the dynamics.

and in particular on the full history of the system, giving rise to a non-Markovian description of the spin properties. Since we use the MF Eq. (5), we call this theory mean-field dissipative spin cooling (MF-DSC).

Using the ansatz in Eq. (10), we can compute $\Pi(\beta_s)$ at all temperatures using standard algorithms based on matrix product states [60, 61]; once this function is determined we can solve the MF-DSC equation:

$$\frac{d}{d\tau} n(\tau) = -4\Gamma \Pi \left(\int_0^\tau n^2 d\tau' \right) n(\tau)^2 \quad (11)$$

using standard Runge-Kutta methods. We compare the time evolution of the gas obtained using our MF-DSC theory with numerical simulations of the master equation using the QuTiP library [48, 49], which are limited in size to $L = 12$. In particular, we simulate the Lindblad master equation in the Zeno limit for the HCFs [17, 20, 47]; the HCF Hamiltonian coincides with the Hubbard model in the $U \rightarrow \infty$ limit: $H' = -t \sum_{j,\sigma} (f_{j,\sigma}^\dagger f_{j+1,\sigma} + \text{H.c.})$; the jump operators read $L'_j = \sqrt{\Gamma/2} \sum_{\mu=\pm 1} (f_{j,\uparrow} f_{j+\mu,\downarrow} - f_{j,\downarrow} f_{j+\mu,\uparrow})$ and follow from the judicious application of the dissipative Schrieffer-Wolff transformation [62, 63] to the original model [17, 20, 47]. Note that for this master equation, the MF Eq. (5) is not valid. Results are shown in Fig. 2 and the agreement is excellent without any fit parameter both for $n(\tau)$ and for $g^{(2)}(\tau)$. We fit a long-time scaling $n(\tau) \sim \tau^{-1/4}$ [not shown in the plot], whereas finite-size simulation are bound to saturate to a finite value.

Inclusion of charge correlations — The inclusion of spatial correlations requires more care. In order to apply our spin-charge decoupling, we observe that the Hamiltonian H' acts only on the charge degrees of freedom and is just a free-fermion model, easily solved in momentum space: $H' = -2t \sum_k \cos k a_k^\dagger a_k$. The Zeno inequality $t \gg \hbar\Gamma$ tells us that the dynamics of the charges is

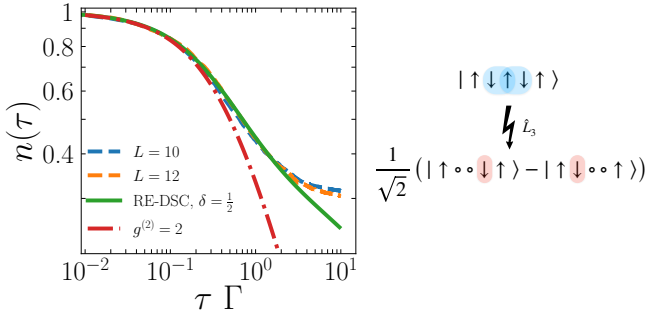


FIG. 3. (Left) Dynamics of the number of particles $n(\tau)$ for an initial $|\Psi_N\rangle$ state. The RE-DSC produces an exceptional description of the process. Dashed-dotted lines indicate the naïve prediction with $g^{(2)} = 2$ kept constant during the dynamics. (Right) Sketch of a loss process taking place on $|\Psi_N\rangle$ at site $j = 4$. In this case, quantum correlations are created only for fermions with spin up (bold and blue arrow), explaining the fact that spatial quantum correlations are created only for one spin species, implying the value $\delta = 1/2$ in (12) for the antiferromagnetic state $|\Psi_N\rangle$.

much faster than the loss rate, and we employ a time-dependent generalised Gibbs ensemble (GGE) approximation for the charge sector [22, 24, 64, 65]. The idea is that at any time τ the charge sector can be described by $\rho_c(\tau) \sim \prod_k e^{-\beta_k(\tau)} a_k^\dagger a_k$, fully determined by the occupation numbers $n_k(\tau) = \langle a_k^\dagger a_k \rangle_\tau$.

Based on previous works on the quantum Zeno effect of bosons, we propose the following rate equations [47]:

$$\frac{dn_k}{d\tau} = -\Gamma g^{(2)} \int_{-\pi}^{\pi} \frac{dq}{2\pi} \left[1 - \delta + \delta (\cos k - \cos q)^2 \right] n_q n_k. \quad (12)$$

Spin physics is taken into account by the $g^{(2)}(\tau)$ but also by the parameter δ , that depends on the spin order of the initial state. Concerning the $g^{(2)}(\tau)$, the rate equations (12) predict that when the initial state has one particle per site, the momentum distribution function takes the form $n_k(\tau) = \alpha_1(\tau) e^{-\delta \alpha_2(\tau) \cos^2(k)}$ at all times [47], where $\alpha_{1,2}(\tau)$ are time-dependent functions that we do not specify. This form of $n_k(\tau)$ implies factorisation of density correlations $\langle n_j n_{j+1} \rangle_\tau = \langle n_j \rangle_\tau \langle n_{j+1} \rangle_\tau = n^2(\tau)$, giving $g^{(2)}(\tau) = 4\Pi(\tau)$; the dynamics of $\Pi(\tau)$ is then computed using the aforementioned method of dissipative spin cooling. Regarding δ , when $\delta = 0$, we obtain the MF-DSC equation (11) of the incoherent spin state by integrating over k ; finite values of δ are necessary to describe time evolution of pure states with generic spin order, as we shall see in the next section. We denote the method based on Eq. (12) the *rate-equation dissipative spin cooling* (RE-DSC).

Antiferromagnetic spin state and charge correlations — As an example, we consider the system initialised in the Néel state $|\Psi_N\rangle$ introduced above, which is a zero-magnetisation eigenstate of $\Sigma^z = \sum_\ell \Sigma_\ell^z$. To correctly describe the dynamics originating from this state,

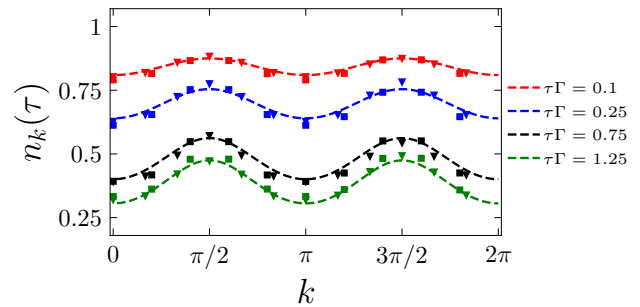


FIG. 4. Momentum distribution function computed from the full numerical solution of the Lindblad master equation for $L = 10$ (squares) and $L = 12$ (triangles) at different times and the predictions by eq. (12).

we need to use the RE-DSC approach; in this case, $\delta = 1/2$. As sketched in Fig. 3(right), a loss process on the Néel state creates a linear superposition of two spin states: while this creates quantum correlation for one spin species, the other one remains uncorrelated; the value $\delta = 1/2$ takes this effect into account. Different states with other spin orders are thus expected to be described by different values of δ . Similar reasoning gives $\delta = 1/8$ for the infinite spin temperature state, explaining this way the use of $\delta = 0$ as a very good approximation for such a state.

We perform exact simulations of the Lindblad dynamics for up to $L = 12$ and compare it with our RE-DSC theory, see Fig. 3(left). We reproduce well the numerical data and we fit a scaling $n(\tau) \sim \tau^{-1/3}$ [not shown in the plot].

An important aspect of the RE-DSC theory is that it also allows to compute the momentum distribution function $n_k(\tau)$, that could be measured in an experiment. In Fig. 4 we present a comparison of the numerical data with the results of our theory; the agreement is excellent and explains very well the appearance of two peaks at $k = \pm\pi/2$, which is a distinctive feature of this Zeno regime of strong losses. Note that the description of these peaks is not possible with the MF-DSC method.

Finally, our theory also gives access to the correlations $g^{(2)}(\tau)$ and predicts an algebraic decay for both the fully-mixed spin state, see Fig. 2(right), and the Néel state, see [47]. This is in contrast with the exponential decay witnessed in numerical simulations of small system sizes. As discussed in Ref. [18], an exponential decay of $g^{(2)}(\tau)$ is necessary to have some population in the stationary state. Our theory addresses the thermodynamic limit of the model, and since the spin $\langle S^2 \rangle$ of the initial state scales as L and not as L^2 , we predict a final vanishing density, which is compatible with the algebraic decay [30]. Moreover, decay of $g^{(2)}(\tau)$ to zero for large τ is compatible with the creation of long-time states whose spin-wavefunction is a Dicke state, which is one of the

most intriguing aspects of this loss process [27, 30].

Conclusions — In this letter, we have presented a theoretical model for the full-time dynamics of a spin-1/2 gas in the presence of two-body losses. Our approach is based on a spin-charge decoupling that holds for strong losses or strong interactions. Our predictions, valid in the thermodynamic limit, highlight the pivotal role of the non-Markovian and non-Hermitian spin dynamics. Our theory goes beyond previous studies by predicting the behaviour in real-time of several observables: density, spin correlations, and momentum distribution function; they could be tested in cold-atom experiments. Concerning its validity, the main approximation is that the spin properties of the gas could be fully described by a non-Hermitian and non-Markovian no-click dynamics. This approximation avoids the need to consider chains of different lengths and turns out to be rather effective; yet, it is not obvious that is valid also at asymptotically long times, and we leave this point for future inspection.

We have focused mainly on the QZ regime, but opposite to it, another regime exists in the parameter space [30]. In non-Hermitian Hamiltonians, the transition between these two regimes is sharp also at finite size and is known as superradiance transition [44]. Concerning the true master equation, whereas these two dynamical behaviours are separated by an intermediate region or are directly in contact, is an open and very intriguing question, left for future work.

Note added — Recently, we became aware of an experimental article studying the dynamics of a SU(6) gas in presence of two-body losses [66]. We believe that methods similar to those presented here could be used to describe that gas in the regime of strong losses.

Acknowledgement — We are grateful to M. Zvonarev for sharing with us his work on the spin-charge separation in the one-dimensional Hubbard model. Uncountable discussions with K. Sponselee on the experimental setup are also gratefully acknowledged. We thank F. Essler for useful discussions on the Hubbard model. This work has been partially funded by LabEx PALM (ANR-10-LABX-0039-PALM) and ERC Starting Grant 101042293 (HEPIQ).

(1999).

- [4] M. Roncaglia, M. Rizzi, and J. I. Cirac, Pfaffian state generation by strong three-body dissipation, *Phys. Rev. Lett.* **104**, 096803 (2010).
- [5] B. Rauer, P. Grīšins, I. E. Mazets, T. Schweigler, W. Rohringer, R. Geiger, T. Langen, and J. Schmiedmayer, Cooling of a one-dimensional bose gas, *Phys. Rev. Lett.* **116**, 030402 (2016).
- [6] M. Schemmer and I. Bouchoule, Cooling a bose gas by three-body losses, *Phys. Rev. Lett.* **121**, 200401 (2018).
- [7] L. H. Dogra, J. A. P. Glidden, T. A. Hilker, C. Eigen, E. A. Cornell, R. P. Smith, and Z. Hadzibabic, Can three-body recombination purify a quantum gas?, *Phys. Rev. Lett.* **123**, 020405 (2019).
- [8] I. Bouchoule and J. Dubail, Breakdown of tan's relation in lossy one-dimensional bose gases, *Phys. Rev. Lett.* **126**, 160603 (2021).
- [9] B. Laburthe Tolra, K. M. O'Hara, J. H. Huckans, W. D. Phillips, S. L. Rolston, and J. V. Porto, Observation of reduced three-body recombination in a correlated 1d degenerate bose gas, *Phys. Rev. Lett.* **92**, 190401 (2004).
- [10] N. Syassen, D. M. Bauer, M. Lettner, T. Volz, D. Dietze, J. J. García-Ripoll, J. I. Cirac, G. Rempe, and S. Dürr, Strong dissipation inhibits losses and induces correlations in cold molecular gases, *Science* **320**, 1329 (2008).
- [11] E. Haller, M. Rabie, M. J. Mark, J. G. Danzl, R. Hart, K. Lauber, G. Pupillo, and H.-C. Nägerl, Three-body correlation functions and recombination rates for bosons in three dimensions and one dimension, *Phys. Rev. Lett.* **107**, 230404 (2011).
- [12] L. Franchi, L. F. Livi, G. Cappellini, G. Binella, M. Inguscio, J. Catani, and L. Fallani, State-dependent interactions in ultracold ^{174}yb probed by optical clock spectroscopy, *New J. Phys.* **19**, 103037 (2017).
- [13] R. Bouganne, M. B. Aguilera, A. Dereau, E. Soave, J. Beugnon, and F. Gerbier, Clock spectroscopy of interacting bosons in deep optical lattices, *New J. Phys.* **19**, 113006 (2017).
- [14] T. Tomita, S. Nakajima, I. Danshita, Y. Takasu, and Y. Takahashi, Observation of the mott insulator to superfluid crossover of a driven-dissipative bose-hubbard system, *Sci. Adv.* **3**, e1701513 (2017).
- [15] T. Tomita, S. Nakajima, Y. Takasu, and Y. Takahashi, Dissipative bose-hubbard system with intrinsic two-body loss, *Phys. Rev. A* **99**, 031601 (2019).
- [16] B. Yan, S. A. Moses, B. Gadway, J. Covey, K. R. A. Hazzard, A. M. Rey, D. S. Jin, and J. Ye, *Nature* **501**, 521 (2013).
- [17] B. Zhu, B. Gadway, M. Foss-Feig, J. Schachenmayer, M. L. Wall, K. R. A. Hazzard, B. Yan, S. A. Moses, J. P. Covey, D. S. Jin, J. Ye, M. Holland, and A. M. Rey, Suppressing the loss of ultracold molecules via the continuous quantum zeno effect, *Phys. Rev. Lett.* **112**, 070404 (2014).
- [18] K. Sponselee, L. Freystatzky, B. Abeln, M. Diem, B. Hundt, A. Kochanke, T. Ponath, B. Santra, L. Mathey, K. Sengstock, and C. Becker, Dynamics of ultracold quantum gases in the dissipative fermi-hubbard model, *Quantum Sci. Technol.* **4**, 014002 (2019).
- [19] S. K. Baur and E. J. Mueller, Two-body recombination in a quantum-mechanical lattice gas: Entropy generation and probing of short-range magnetic correlations, *Phys. Rev. A* **82**, 023626 (2010).

* leonardo.mazza@universite-paris-saclay.fr

- [1] Y. Kagan, B. V. Svistunov, and G. V. Shlyapnikov, Effect of bose condensation on inelastic processes in gases, *Pis'ma Zh. Eksp. Teor. Fiz.* **42**, 169 (1985).
- [2] E. A. Burt, R. W. Ghrist, C. J. Myatt, M. J. Holland, E. A. Cornell, and C. E. Wieman, Coherence, correlations, and collisions: What one learns about bose-einstein condensates from their decay, *Phys. Rev. Lett.* **79**, 337 (1997).
- [3] J. Söding, D. Guéry-Odelin, P. Desbiolles, F. Chevy, H. Inamori, and J. Dalibard, *Appl. Phys. B* **69**, 257

[20] J. J. García-Ripoll, S. Dürr, N. Syassen, D. M. Bauer, M. Lettner, G. Rempe, and J. I. Cirac, Dissipation-induced hard-core boson gas in an optical lattice, *New J. Phys.* **11**, 013053 (2009).

[21] I. Bouchoule, B. Doyon, and J. Dubail, The effect of atom losses on the distribution of rapidities in the one-dimensional Bose gas, *SciPost Phys.* **9**, 44 (2020).

[22] D. Rossini, A. Ghermaoui, M. B. Aguilera, R. Vatré, R. Bouganne, J. Beugnon, F. Gerbier, and L. Mazza, Strong correlations in lossy one-dimensional quantum gases: From the quantum zeno effect to the generalized gibbs ensemble, *Phys. Rev. A* **103**, L060201 (2021).

[23] I. Bouchoule, L. Dubois, and L.-P. Barbier, Losses in interacting quantum gases: Ultraviolet divergence and its regularization, *Phys. Rev. A* **104**, L031304 (2021).

[24] L. Rosso, A. Biella, and L. Mazza, The one-dimensional Bose gas with strong two-body losses: the effect of the harmonic confinement, *SciPost Phys.* **12**, 44 (2022).

[25] L. Rosso, L. Mazza, and A. Biella, Eightfold way to dark states in $su(3)$ cold gases with two-body losses, *Phys. Rev. A* **105**, L051302 (2022).

[26] O. Scarlatella, A. A. Clerk, R. Fazio, and M. Schiró, Dynamical mean-field theory for markovian open quantum many-body systems, *Phys. Rev. X* **11**, 031018 (2021).

[27] M. Foss-Feig, A. J. Daley, J. K. Thompson, and A. M. Rey, Steady-state many-body entanglement of hot reactive fermions, *Phys. Rev. Lett.* **109**, 230501 (2012).

[28] M. Nakagawa, N. Tsuji, N. Kawakami, and M. Ueda, Dynamical sign reversal of magnetic correlations in dissipative hubbard models, *Phys. Rev. Lett.* **124**, 147203 (2020).

[29] M. Nakagawa, N. Kawakami, and M. Ueda, Exact liouvillian spectrum of a one-dimensional dissipative hubbard model, *Phys. Rev. Lett.* **126**, 110404 (2021).

[30] L. Rosso, D. Rossini, A. Biella, and L. Mazza, One-dimensional spin-1/2 fermionic gases with two-body losses: Weak dissipation and spin conservation, *Phys. Rev. A* **104**, 053305 (2021).

[31] B. Misra and E. C. G. Sudarshan, The zeno's paradox in quantum theory, *J. Math. Phys.* **18**, 756 (1977).

[32] W. M. Itano, D. J. Heinzen, J. J. Bollinger, and D. J. Wineland, Quantum zeno effect, *Phys. Rev. A* **41**, 2295 (1990).

[33] A. Beige, D. Braun, B. Tregenna, and P. L. Knight, Quantum computing using dissipation to remain in a decoherence-free subspace, *Phys. Rev. Lett.* **85**, 1762 (2000).

[34] A. Beige, D. Braun, and P. L. Knight, Driving atoms into decoherence-free states, *New J. Phys.* **2**, 22 (2000).

[35] J. Kempe, D. Bacon, D. A. Lidar, and K. B. Whaley, Theory of decoherence-free fault-tolerant universal quantum computation, *Phys. Rev. A* **63**, 042307 (2001).

[36] P. Facchi, H. Nakazato, and S. Pascazio, From the quantum zeno to the inverse quantum zeno effect, *Phys. Rev. Lett.* **86**, 2699 (2001).

[37] P. Facchi and S. Pascazio, Quantum zeno subspaces, *Phys. Rev. Lett.* **89**, 080401 (2002).

[38] R. Schützhold and G. Gnanapragasam, Quantum zeno suppression of three-body losses in bose-einstein condensates, *Phys. Rev. A* **82**, 022120 (2010).

[39] K. Stannigel, P. Hauke, D. Marcos, M. Hafezi, S. Diehl, M. Dalmonte, and P. Zoller, Constrained dynamics via the zeno effect in quantum simulation: Implementing non-abelian lattice gauge theories with cold atoms, *Phys. Rev. Lett.* **112**, 120406 (2014).

[40] Z. Gong, S. Higashikawa, and M. Ueda, Zeno hall effect, *Phys. Rev. Lett.* **118**, 200401 (2017).

[41] H. Fröml, C. Muckel, C. Kollath, A. Chiocchetta, and S. Diehl, Ultracold quantum wires with localized losses: Many-body quantum zeno effect, *Phys. Rev. B* **101**, 144301 (2020).

[42] K. Snizhko, P. Kumar, and A. Romito, Quantum zeno effect appears in stages, *Phys. Rev. Research* **2**, 033512 (2020).

[43] A. Biella and M. Schiró, Many-Body Quantum Zeno Effect and Measurement-Induced Subradiance Transition, *Quantum* **5**, 528 (2021).

[44] Y. Ashida, Z. Gong, and M. Ueda, Non-hermitian physics, *Advances in Physics* **69**, 249 (2020).

[45] P. Weinberg and M. Bukov, QuSpin: a Python Package for Dynamics and Exact Diagonalisation of Quantum Many Body Systems part I: spin chains, *SciPost Phys.* **2**, 003 (2017).

[46] P. Weinberg and M. Bukov, QuSpin: a Python Package for Dynamics and Exact Diagonalisation of Quantum Many Body Systems. Part II: bosons, fermions and higher spins, *SciPost Phys.* **7**, 20 (2019).

[47] L. Rosso, A. Biella, J. De Nardis, and L. Mazza, Supplemental material, URL will be inserted by the publisher.

[48] J. Johansson, P. Nation, and F. Nori, Qutip: An open-source python framework for the dynamics of open quantum systems, *Computer Physics Communications* **183**, 1760 (2012).

[49] J. Johansson, P. Nation, and F. Nori, Qutip 2: A python framework for the dynamics of open quantum systems, *Computer Physics Communications* **184**, 1234 (2013).

[50] M. Ogata and H. Shiba, Bethe-ansatz wave function, momentum distribution, and spin correlation in the one-dimensional strongly correlated hubbard model, *Phys. Rev. B* **41**, 2326 (1990).

[51] M. Noga, Separation of charge and spin degrees of freedom in the hubbard model, *Czech. J. Phys.* **42**, 823 (1992).

[52] S. Östlund and M. Granath, Exact transformation for spin-charge separation of spin-1/2 fermions without constraints, *Phys. Rev. Lett.* **96**, 066404 (2006).

[53] B. Kumar, Canonical representation for electrons and its application to the hubbard model, *Phys. Rev. B* **77**, 205115 (2008).

[54] B. Kumar, Exact solution of the infinite- u hubbard problem and other models in one dimension, *Phys. Rev. B* **79**, 155121 (2009).

[55] A. Montorsi and M. Roncaglia, Nonlocal order parameters for the 1d hubbard model, *Phys. Rev. Lett.* **109**, 236404 (2012).

[56] A. Nocera, F. H. L. Essler, and A. E. Feiguin, Finite-temperature dynamics of the mott insulating hubbard chain, *Phys. Rev. B* **97**, 045146 (2018).

[57] E. Tartaglia, P. Calabrese, , and B. Bertini, Real-Time Evolution in the Hubbard Model with Infinite Repulsion, *SciPost Phys.* **12**, 28 (2022).

[58] M. Zvonarev, private communication, article in preparation.

[59] A. Sergi and K. G. Zloshchastiev, Time correlation functions for non-hermitian quantum systems, *Phys. Rev. A* **91**, 062108 (2015).

- [60] U. Schollwöck, The density-matrix renormalization group in the age of matrix product states, *Annals of Physics* **326**, 96 (2011).
- [61] M. Fishman, S. R. White, and E. M. Stoudenmire, The ITensor software library for tensor network calculations, (2020), arXiv:2007.14822.
- [62] T. Kato, *Perturbation theory for linear operators*, edited by Springer (1995).
- [63] E. M. Kessler, Generalized schrieffer-wolff formalism for dissipative systems, *Phys. Rev. A* **86**, 012126 (2012).
- [64] F. Lange, Z. Lenarčič, and A. Rosch, Time-dependent generalized gibbs ensembles in open quantum systems, *Phys. Rev. B* **97**, 165138 (2018).
- [65] K. Mallayya, M. Rigol, and W. De Roeck, Prethermalization and thermalization in isolated quantum systems, *Phys. Rev. X* **9**, 021027 (2019).
- [66] K. Honda, S. Taie, Y. Takasu, N. Nishizawa, M. Nakagawa, and Y. Takahashi, Observation of the sign reversal of the magnetic correlation in a driven-dissipative fermi-hubbard system (2022), arXiv:2205.13162.

Supplementary Material

A dynamical theory for one-dimensional fermions with strong two-body losses: universal non-Hermitian Zeno physics and spin-charge separation

Lorenzo Rosso¹, Alberto Biella^{2,1}, Jacopo De Nardis³ and Leonardo Mazza¹

¹Université Paris-Saclay, CNRS, LPTMS, 91405 Orsay, France

²INO-CNR BEC Center and Dipartimento di Fisica, Università di Trento, 38123 Povo, Italy

³Laboratoire de Physique Théorique et Modélisation, CNRS UMR 8089, CY Cergy Paris Université, 95302 Cergy-Pontoise Cedex, France

CONTENTS

A. Details about the phase diagram	8
B. Mean-field universality	8
C. Derivation of the effective master equation for hard-core fermions	9
First-order corrections: hard-core fermions	9
Second-order corrections	9
D. Derivation of the rate equations - Eq. (12) of the main text	10
E. Details on the self-consistent numerical solution of the rate equations with the spin dynamics	12

Appendix A: Details about the phase diagram

In this section we present additional numerical data concerning the properties of the non-Hermitian Hamiltonian \tilde{H} associated to our model. In the main text we have stressed the fact that \tilde{H} is a powerful tool that allows us to characterise the transient dynamics in the whole parameter space by focusing on its complex eigenvalues. In particular, one can identify two main region: a mean-field (MF) and a quantum-Zeno (QZ) one.

In Fig. S1 we show a cut in the phase diagram of the model at fixed U/t (top) and at fixed $\hbar\gamma/t$ (bottom). The top panel clearly shows a region up to $\hbar\gamma/t \sim 10$ where the imaginary part increases linearly with γ : we interpret this as the MF region. On the other hand, for $\hbar\gamma/t \gtrsim 3$ the spectrum starts to split in two parts: a linearly increasing, and a subradiant one, which is the smoking gun of the QZ effect.

Moreover, the bottom panel of Fig. S1 shows that the QZ regime can be achieved even for weak dissipation just by increasing the interactions. The latter observation corresponds to our claim in the main text: it is the modulus of the adimensional complex interaction $|\xi|$ that identifies whether we are in the MF or QZ regime.

As we mention in the conclusions of the article, a thorough investigation of the model in the whole phase space is particularly interesting, and could help understanding whether another transient behaviour is “hidden” between the MF and QZ regimes.

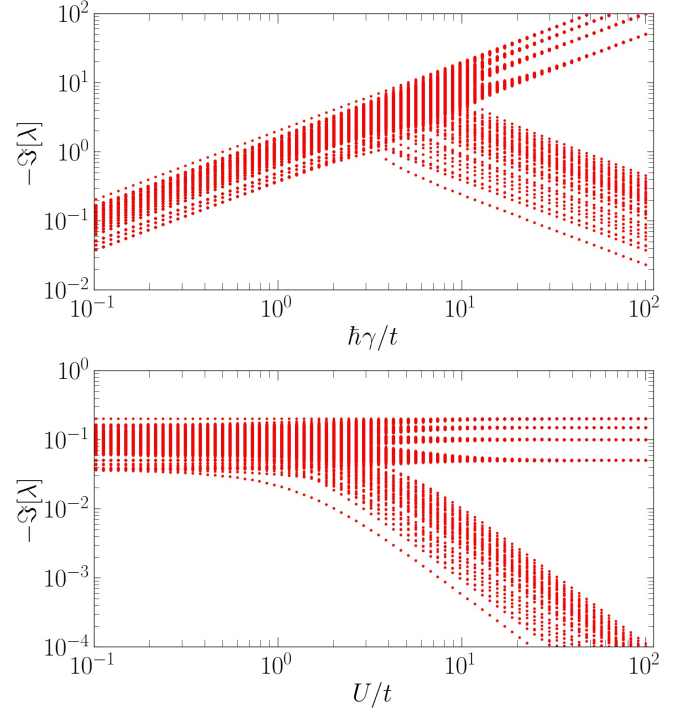


FIG. S1. Imaginary part (with reversed sign) of the eigenvalues of the non-Hermitian Hamiltonian in the sector with $N = L = 8$ and $S_Z = 0$. Top panel: vertical cut in the phase diagram of Fig. 1 of the main text at $U = 0$. Bottom panel: horizontal cut in the phase diagram of Fig. 1 of the main text at $\hbar\gamma = 0.1$.

Appendix B: Mean-field universality

In the weakly-dissipative and weakly-interacting mean-field regime appearing approximately for $|\xi| \lesssim 2.0$, the imaginary part of the eigenvalues increases linearly with γ , so that the lifetime of the gas decreases by increasing the loss rate (see Fig. S1 top panel). To quantify this behaviour, we define

$$\bar{\zeta} = \frac{\sum_i \Im[\lambda_i]}{\hbar\gamma} \quad (B1)$$

where λ_i are the eigenvalues of \tilde{H} and the sum is restricted to a set of eigenvalues with smallest imaginary part (in absolute value), which are those that determine the long-time dynamics. The plot in Fig. S2 shows that $\bar{\zeta}$ has a clear finite value in a finite parameter region. In

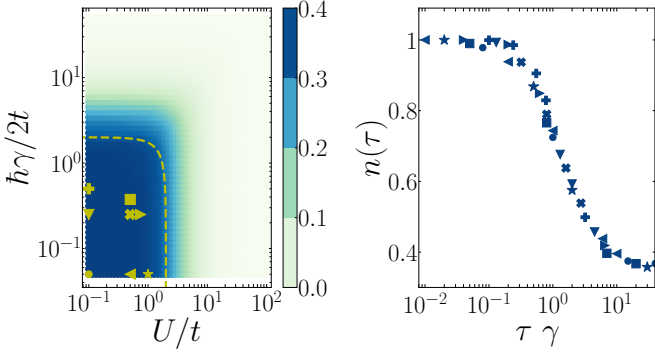


FIG. S2. (Left) Color plot of $\bar{\zeta}$ in the parameter space. The green dashed line is the circumference with radius $|\xi| = 2.0$ and is proposed as an approximate bound for the QZ regime. The exact diagonalisation is performed for $N = L = 8$ in the sector $S_z = 0$ magnetisation. (Right) Universal MF dynamics for the density of the gas: different symbols correspond to different points in the MF region of the parameter space. The collapse is obtained by rescaling time with γ . Simulations are performed for $L = 6$.

the right panel of Fig. S2 we show the collapse of the curves by the appropriate rescaling with γ .

Appendix C: Derivation of the effective master equation for hard-core fermions

In this section we present some details about the derivation of the effective master equation governing the dynamics in the quantum Zeno regime analyzed in the main text, that was called $\dot{\rho} = \mathcal{L}'[\rho]$. We follow the method employed in Ref [20]; the final result has already been presented in Ref. [17] without derivation.

We regroup the terms of the master equation

$$\frac{d\rho}{d\tau} = (\mathcal{V} + \mathcal{L}_{int})\rho \quad (C1)$$

in the following manner:

$$\mathcal{V}[\rho] = -\frac{i}{\hbar}[H_t, \rho], \quad \mathcal{L}_{int}[\rho] = -\frac{i}{\hbar}[H_U, \rho] + \mathcal{D}[\rho] \quad (C2)$$

where the Hamiltonians are:

$$H_t = -t \sum_{j,\sigma} \left(c_{j,\sigma}^\dagger c_{j+1,\sigma} + H.c. \right), \quad H_U = U \sum_j n_{j,\uparrow} n_{j,\downarrow} \quad (C3)$$

and the dissipation is:

$$\mathcal{D}[\rho] = \sum_j L_j \rho L_j^\dagger - \frac{1}{2} \left\{ L_j^\dagger L_j, \rho \right\}, \quad L_j = \sqrt{\gamma} c_{j,\uparrow} c_{j,\downarrow} \quad (C4)$$

This rewriting is useful to highlight the different orders of magnitude of the various term: \mathcal{V} is a perturbation of order t , and we assume that in the quantum Zeno limit $|U - i\hbar\gamma/2| \gg t$. In the following we are going to tackle the problem by means of a perturbative approach.

Let us start by focusing on the properties of \mathcal{L}_{int} , a non-Hermitian operator with infinitely many eigenstates. Exploiting a generalized version of Kato's method [62] it is possible to expand: $\mathcal{L}_{int} = \sum_i \lambda_i \mathcal{P}_i$, using a complete set of projector operators with the following properties:

$$\mathcal{P}_i \mathcal{P}_j = \delta_{ij} \mathcal{P}_i, \quad \sum_i \mathcal{P}_i = 1. \quad (C5)$$

\mathcal{P}_0 projects the density-matrix over the hard-core fermion (HCF) subspace, which is stable. We call ρ_0 the density matrix restricted to the subspace. With perturbative techniques, it is now possible to construct the effective master equation governing the dynamics for the dominant term $\rho_0(t)$:

$$\frac{d}{d\tau} \rho_0 = (\mathcal{L}_1 + \mathcal{L}_2) \rho_0 \quad (C6)$$

with

$$\mathcal{L}_1 = \mathcal{P}_0 \mathcal{L}_{int} \mathcal{P}_0; \quad \mathcal{L}_2 = \sum_c -\frac{1}{\lambda_c} \mathcal{P}_0 \mathcal{V} \mathcal{P}_c \mathcal{V} \mathcal{P}_0. \quad (C7)$$

First-order corrections: hard-core fermions

Let us start by analyzing the first order corrections given by \mathcal{L}_1 . It can be shown [20] that \mathcal{L}_1 is equivalent to a Hamiltonian that has been projected within states without double occupancies. This is precisely a hard-core fermion gas under unitary Hamiltonian evolution $\mathcal{L}_1[\rho_0] = -\frac{i}{\hbar}[H', \rho_0]$ where

$$H' = -t \sum_{i=1} (f_{i+1\sigma}^\dagger f_{i\sigma} + H.c.) \quad (C8)$$

where $f_{i\sigma}^\dagger$ and $f_{i\sigma}$ are the HCF operators satisfying the Clifford algebra plus the hard-core constraint. The main result so far is that two body losses in the strongly dissipative regime lead to a coherent dynamics given by an hard-core fermion Hamiltonian.

Second-order corrections

The second order Liouville can be recasted in a Lindblad form:

$$\mathcal{L}_2[\rho_0] = \frac{i}{\hbar} [H'_2, \rho_0] + \mathcal{D}_2[\rho_0], \quad (C9)$$

where:

$$H'_2 = -t_2 \sum_j L'_j L'_j; \quad (C10a)$$

$$\mathcal{D}_2[\rho_0] = \sum_j L'_j \rho_0 L'^\dagger_j - \frac{1}{2} \left\{ L'^\dagger_j L'_j, \rho_0 \right\}. \quad (C10b)$$

The new set of jump operators describing the lossy dynamics is thus given by:

$$L'_i = \sqrt{\frac{\Gamma}{2}} [(f_{i,\uparrow}f_{i+1,\downarrow} - f_{i,\downarrow}f_{i+1,\uparrow}) + (f_{i,\uparrow}f_{i-1,\downarrow} - f_{i,\downarrow}f_{i-1,\uparrow})], \quad (\text{C11})$$

with the coefficients given by:

$$t_2 = \frac{4t^2U}{\hbar^2\gamma^2} \frac{1}{1 + \left(\frac{2U}{\hbar\gamma}\right)^2} = \frac{U}{|\xi|}, \quad \Gamma = \frac{4t^2}{\hbar^2\gamma} \frac{1}{1 + \left(\frac{2U}{\hbar\gamma}\right)^2} = \frac{\gamma}{|\xi|}, \quad (\text{C12})$$

where we recall $\xi = U/t - i\hbar\gamma/2t$ is the adimensional complex interaction defined in the main text.

Concluding, the effective master equation for the HCF has the following form (we dismiss here the notation ρ_0 , that is not used in the main text):

$$\frac{d}{d\tau} \rho(\tau) = -\frac{i}{\hbar} [H' + H'_2, \rho(\tau)] + \sum_j \left[L'_j \rho(\tau) L'_j - \frac{1}{2} \{ L'_j L'_j, \rho(\tau) \} \right]. \quad (\text{C13})$$

In the main text we do not make any explicit mention to H'_2 because it is completely irrelevant in the study that we carry out. This of course depends on the specific problem that we have chose to address, and this could not be the case for other situations.

Appendix D: Derivation of the rate equations - Eq. (12) of the main text

In this section we consider the effective master equation for HCF that we have derived in Sec. C. Our goal is to present a derivation of the rate equations that appear in Eq. (12) of the main text.

As we said in the main text, the Hamiltonian H' has

a simple form in the language of spin-charge separation:

$$H' = -t \sum_j (a_j^\dagger a_{j+1} + H.c.) = -2t \sum_k \cos k a_k^\dagger a_k. \quad (\text{D1})$$

Similarly to what has been done for bosons in Ref. [22] we propose a generalised-Gibbs ensemble:

$$\rho_c(\tau) = \prod_k \frac{e^{-\beta_k(\tau)a_k^\dagger a_k}}{\mathcal{Z}_k(\tau)} \quad (\text{D2})$$

fully determined by the occupation numbers $n_k(\tau) = \langle a_k^\dagger a_k \rangle_\tau$. Using the master equation, we can take the time-derivative of $n_k(t) = \text{Tr} [a_k^\dagger a_k \rho(t)]$, that reads:

$$\frac{d}{d\tau} n_k(\tau) = \frac{i}{\hbar} \left\langle [H' + H'_2, a_k^\dagger a_k] \right\rangle_t + \sum_j \left\langle L'_j a_k^\dagger a_k L'_j - \frac{1}{2} \{ L'_j L'_j, a_k^\dagger a_k \} \right\rangle_t. \quad (\text{D3})$$

This expression can be simplified. First, we observe that $[H', a_k^\dagger a_k] = 0$; in fact, a more general relation holds, $\langle [A, n_k] \rangle_\tau = 0$, that is valid for any operator A . Indeed:

$$\langle [A, n_k] \rangle_\tau = \text{Tr} [\rho(\tau) A n_k] - \text{Tr} [\rho(\tau) n_k A] \quad (\text{D4})$$

but since $[n_k, \rho_c(\tau)] = 0$, using the cyclic property of the trace we obtain the result. The latter statement is true also for $A = H'_2$: neither of the two Hamiltonians influences the charge dynamics.

Focusing on dissipation, we write:

$$-\sum_j \frac{1}{2} \{ L'_j L'_j, a_k^\dagger a_k \} = -\sum_j L'_j L'_j a_k^\dagger a_k + \frac{1}{2} [L'_j L'_j, a_k^\dagger a_k] \quad (\text{D5})$$

and we obtain:

$$\frac{d}{d\tau} n_k(\tau) = \left\langle \sum_j L'_j \left[a_k^\dagger a_k, L'_j \right] \right\rangle_\tau. \quad (\text{D6})$$

In order to continue, we need to give an expression to L'_j in the spin-charge language. We propose the following one:

$$L'_j = \sqrt{\frac{\Gamma}{2}} \Lambda_j a_j (a_{j-1} + a_{j+1}) \quad (\text{D7})$$

where Λ_j is a complicated non-local object acting both on spin and on charge that we are not able to treat exactly. The role of Λ_j is to check that not only two particles come close by, but that they are also in a spin-singlet: this condition is necessary for a loss event to occur.

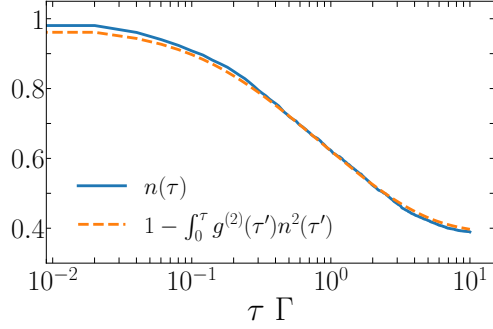


FIG. S3. Exact numerical simulations of the Zeno master equation for the time evolution of an initial spin-incoherent state for $L = 10$. By computing directly $n(\tau)$ and $g^2(\tau)$, we show that $\dot{n}(\tau) = -\Gamma g^{(2)}(\tau)n(\tau)^2$ by integrating over time both members and comparing them.

At this stage, we find impossible to continue our work in an exact way. To begin with, we discuss what happens if we perform two “reasonable” approximations: first, that Λ_j acts only on spin degrees of freedom, and second, that it simply checks whether two neighboring particles are in a spin-singlet channel. In particular, since we cannot say which one is the particle that is annihilated at position j , we will assume that it measures the average number of spin-singlets in the system:

$$\Lambda_j^\dagger \Lambda_j \simeq \frac{1}{N} \sum_\ell \Pi_{\ell, \ell+1}, \quad \forall j. \quad (\text{D8})$$

Note that Λ_j now commutes with any charge degree of freedom. These approximations are sufficient to continue our study.

The state (D2) satisfies Wick’s theorem:

$$\langle c_z^\dagger c_w^\dagger c_k c_q \rangle_\tau = \langle c_z^\dagger c_q \rangle_\tau \langle c_w^\dagger c_k \rangle_\tau - \langle c_z^\dagger c_k \rangle_\tau \langle c_w^\dagger c_q \rangle_\tau \quad (\text{D9})$$

and factorization in momentum space: $\langle c_z^\dagger c_q \rangle_\tau = \delta_{z,q} n_q(\tau)$, so that:

$$\langle c_z^\dagger c_w^\dagger c_k c_q \rangle_\tau = (\delta_{z,q} \delta_{w,k} - \delta_{z,k} \delta_{w,q}) n_q(\tau) n_k(\tau); \quad (\text{D10a})$$

$$\langle c_z^\dagger c_w^\dagger c_k c_q \rangle_\tau - \langle c_q^\dagger c_k^\dagger c_w c_z \rangle_\tau = 0. \quad (\text{D10b})$$

Within the t-GGE approximation Starting from the following formula:

$$\begin{aligned} n_k L'_j &= \Lambda_j n_k \sqrt{\frac{\Gamma}{2}} \frac{1}{L} \sum_{w,q} e^{i(q+w)j} 2 \cos(w) a_w a_q = \\ &= \Lambda_j \sqrt{\frac{\Gamma}{2}} \frac{1}{L} \sum_{w,q} e^{i(q+w)j} 2 \cos(w) a_w a_q (n_k - \delta_{k,w} - \delta_{k,q}), \end{aligned} \quad (\text{D11})$$

we obtain:

$$[n_k, L'_j] = -\sqrt{\frac{\Gamma}{2}} \frac{2}{L} \Lambda_j \sum_q e^{i(q+k)j} (\cos(k) - \cos(q)) a_k a_q; \quad (\text{D12})$$

from which:

$$L'_j^\dagger [n_k, L'_j] = -\frac{2\Gamma}{L^2} \Lambda_j^\dagger \Lambda_j \sum_{q,w,z} e^{i(q+k)j} (\cos(k) - \cos(q)) \cos(w) a_z^\dagger a_w^\dagger a_k a_q. \quad (\text{D13})$$

If we now sum over j we are left with an expression where spin and charge are well separated:

$$\sum_j L'_j^\dagger [n_k, L'_j] = -\frac{2\Gamma}{L^2} \left(\frac{1}{N} \sum_\ell \Pi_{\ell, \ell+1} \right) \sum_{q,w,z} \delta_{k+q, w+z} (\cos(k) - \cos(q)) \cos(w) a_z^\dagger a_w^\dagger a_k a_q. \quad (\text{D14})$$

Moving to expectation values, we get:

$$\begin{aligned} \frac{d}{d\tau} n_k(\tau) &= -\frac{2\Gamma}{L} \Pi(\tau) \sum_q (\cos(k) - \cos(q))^2 n_q(\tau) n_k(\tau) = \\ &= -2\Gamma \Pi(\tau) \int_{-\pi}^{+\pi} \frac{dq}{2\pi} (\cos(k) - \cos(q))^2 n_q(\tau) n_k(\tau). \end{aligned} \quad (\text{D15})$$

Yet, at a more careful analysis, one finds that it is possible to give a better description of the dynamics by mixing the obtained rate equations with a mean-field behaviour:

$$\frac{d}{d\tau} n_k(\tau) = -2\Gamma \Pi(\tau) \int_{-\pi}^{+\pi} \frac{dq}{2\pi} [(1 - \delta) + \delta(\cos(k) - \cos(q))^2] n_q(\tau) n_k(\tau). \quad (\text{D16})$$

Choosing a value of δ in the interval $[0, 1]$ allows to tune

the importance of the mean-field behaviour with respect

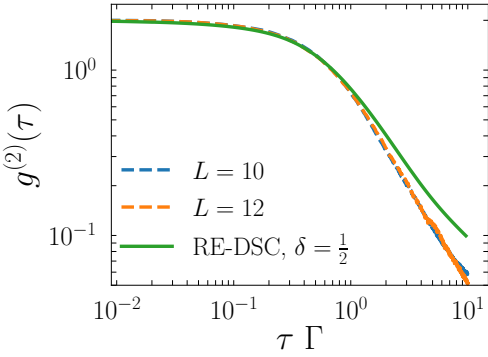


FIG. S4. Dashed lines: exact numerical results for the time evolution of $g^{(2)}$ for the ordered Néel state for $L = 10, 12$. Solid line: theoretical prediction with $\delta = 1/2$

to the correlated one that we just derived. In Fig. S3, for instance, we numerically solve the Zeno master equation and we show that for an initially uncorrelated state the exact numerical data are well described by the mean-field equation $\dot{n} = -\Gamma g^{(2)}n^2$. This is not true when we consider an initial Néel antiferromagnetic state.

In order to understand why we need to use $\delta = 1/2$ for the Néel state, it is useful to observe what happens when we apply a jump operator to $|\uparrow\downarrow\uparrow\downarrow\uparrow\downarrow\rangle$; if we consider $j = 3$, the state is turned into a linear superposition:

$$\frac{|\uparrow\circ\circ\downarrow\uparrow\downarrow\rangle - |\uparrow\downarrow\circ\circ\uparrow\downarrow\rangle}{\sqrt{2}}, \quad (\text{D17})$$

see also the sketch in the main text. Now, it is easy to see that if we compute the momentum distribution function for spins \uparrow , $n_{k,\uparrow} = n_\uparrow = 1/3$. The other spin component, instead, features spatial correlations: $n_{k,\downarrow} = n_\downarrow - \cos(2k)$. In this case, the spins \uparrow do not develop any spatial correlations, and for them a simple mean-field equation would be sufficient. On the other hand, the spins \downarrow feature spatial correlation; of course, the situation would be reverted if the jump operator had acted on another site. This motivates the use of $\delta = 1/2$, that interpolates between these two behaviours, in order to describe the average dissipative dynamics of the system.

We show in Fig. S4 the numerical data for $g^{(2)}(\tau)$ computed from the full numerical solution of the master equation starting from a Néel state, the data are in good agreement, up to finite-size effects, with our theoretical prediction obtained solving Eq. (D16) with $\delta = 1/2$. For a comparison for both the population density $n(\tau)$ and the momentum distribution function $n_k(\tau)$ starting from a Néel state see Fig. 3,4 of the main text. The details about the numerical solution of Eq. (D16) are presented in the next section App. E.

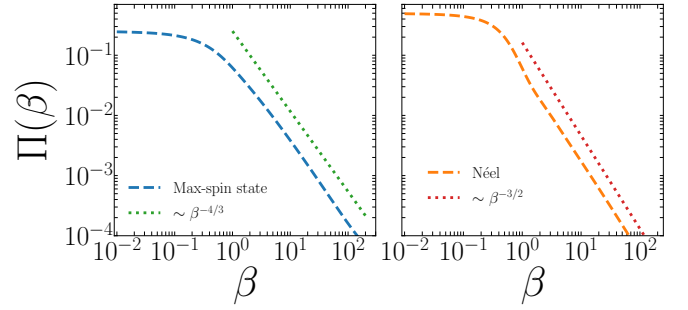


FIG. S5. Non-Hermitian evolution for the spin-singlet projection operator for a (left) maximally-mixed spin state and (right) an ordered Néel state. Dashed lines: MPS data of the non-Hermitian Heisenberg evolution. Dotted lines: long-time behaviour.

Appendix E: Details on the self-consistent numerical solution of the rate equations with the spin dynamics

In order to solve the rate equations for the charge in (D15) that is Eq. (9) in the main text while solving self-consistently the spin dynamics, we need to consider the spin dynamics. The non-Hermitian spin dynamics is governed by a ferromagnetic Heisenberg Hamiltonian, namely:

$$H_s = -\frac{\Gamma}{2} \sum_{\ell} \vec{\Sigma}_{\ell} \cdot \vec{\Sigma}_{\ell+1}; \quad \Gamma > 0. \quad (\text{E1})$$

Within this framework [59], we propose the following ansatz for the density matrix for the spin degrees of freedom:

$$\rho_s(\tau) = \frac{e^{-\beta_s(\tau)H_s}}{\text{Tr} [e^{-2\beta_s(\tau)H_s} \rho(0)]} \rho(0) e^{-\beta_s(\tau)H_s}, \quad (\text{E2})$$

where $\rho(0)$ is the initial spin state, and in the article we have explicitly considered $\rho(0) = \mathbf{1}/d$ (with d a normalization constant) for the maximally-mixed spin state, and $\rho(0) = |\Psi_{\text{Néel}}\rangle\langle\Psi_{\text{Néel}}|$ for the ordered Néel state.

We employ matrix-product-states based algorithm to reconstruct the expectation value of the operator

$$\frac{1}{N} \sum_{\ell} \Pi_{\ell,\ell+1} \quad (\text{E3})$$

for every value of β_s , so that the function $\Pi(\beta)$ is obtained; two examples are given in Fig. (S5).

The dynamics of $\beta_s(\tau)$ is given by:

$$\begin{aligned} \beta_s(\tau) &= \frac{1}{L} \sum_j \int_0^\tau \langle n_j n_{j+1} \rangle(\tau') d\tau' = \\ &= \int_0^t d\tau' \int_{-\pi}^\pi \frac{dq}{2\pi} \int_{-\pi}^\pi \frac{dk}{2\pi} n_k n_q (1 - \cos(q - k)). \end{aligned} \quad (\text{E4})$$

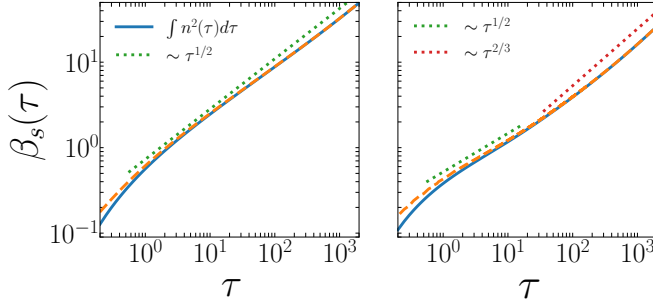


FIG. S6. Time evolution of the effective spin chemical potential $\beta_s(\tau)$ (orange-dashed lines) compared with the time integral of the squared density (blue solid lines) for a maximally-mixed spin state (left) and an ordered Néel state (right). Dotted lines represent the theoretical trends.

The specific value of Π that should be taken at time

τ thus requires the knowledge of the function $\beta_s(\tau)$. This turns the the rate equations into a set of integro-differential equations, for which we propose a numerical approximate solution. We implement a 4th-order Runge-Kutta (RK) algorithm that assumes that $\Pi(\beta)$ is constant during the four intermediate steps of the RK algorithm. First, at fixed τ we compute $\beta_s(\tau)$ according to Eq. (E4), next we use a simple linear interpolation of the MPS data to obtain the value for $\Pi(\tau)$. Once the latter value has been obtained, we run the 4 standard intermediate steps of the RK algorithm. We employ an integration step of $d\tau = 10^{-2}$ and $N_{\text{steps}} = 5 \cdot 10^4$, while we have discretised the k space in 10^2 points in between the range $[0, 2\pi]$, which corresponds to consider a lattice with $L = 100$ sites.

We conclude by displaying the data in Fig. S6, which show the evolution of β_s as a function of time.